Unraveling strongly entropic effect on β-relaxation in metallic glass: Insights from enhanced atomistic samplings over experimentally relevant timescales

Yi-Bo Yang,[1,2,*] Qun Yang,[3] Dan Wei,[1] Lan-Hong Dai,[1,4] Hai-Bin Yu,[3] and Yun-Jiang Wang[1,4,†]

[1]*State Key Laboratory of Nonlinear Mechanics, Institute of Mechanics, Chinese Academy of Sciences, Beijing 100190, China*

[2]*School of Physical Science, University of Chinese Academy of Sciences, Beijing 100049, China*

[3]*Wuhan National High Magnetic Field Center and School of Physics, Huazhong University of Science and Technology, Wuhan 430074, Hubei, China*

[4]*School of Engineering Science, University of Chinese Academy of Sciences, Beijing 100049, China*

(Received 4 August 2020; revised 15 October 2020; accepted 22 October 2020; published 4 November 2020)

The Johari-Goldstein secondary (β) relaxation is an intrinsic feature of glasses, which is crucial to many properties of disordered materials. One puzzling feature of β-relaxation is its wide relaxation peak, which could imply a critical role of entropy. Here we quantify the activation entropy related to the β-relaxation in metallic glass via well-tempered metadynamics simulations. The activation free energy of the β-relaxation drastically decreases with increasing temperature, indicating a strongly entropic effect that may contribute a multiplication prefactor up to several orders of magnitude to the frequency. We further argue the entropic effect by linear extrapolation of the temperature-dependent activation free energy to 0 K, which gives rise to activation energy, in agreement with the barrier spectrum explored by the activation-relaxation technique. The entropic effect signifies the multiplicity of activation pathways which agrees with the experimentally found wide frequency domain of the β-relaxation.

DOI: 10.1103/PhysRevB.102.174103

I. INTRODUCTION

While it is well known that the dynamic processes in crystalline materials are accommodated by the motion of defects like vacancy, dislocation, boundary, etc., such a scenario breaks down in amorphous solids [1–4]. Since its discovery half a century ago in rigid-molecule glasses, the Johari-Goldstein β-relaxation [5], or the secondary relaxation, has been an intriguing subject in the broad community of glass physics and condensed-matter physics [6–11].

As the primary α-relaxation is frozen below the glass transition temperature, β-relaxation dominates the dynamics of amorphous solids. It plays important roles in several dynamic properties of metallic glasses (MGs), including relaxation and aging [12], rejuvenation [13,14], and elastoviscoplastic deformation [15–18], as well as α-relaxation [19], glass transition [10,20,21], etc. However, the structural origin of β-relaxation still remains elusive [22,23]. A prevalent physical mechanism of β-relaxation originates from the potential energy landscape (PEL) theory [24], which regards it as local barrier crossing events between neighboring basins. The β-relaxation is also believed to be associated with the shear transformation zone, as the β process involves rearrangement of local atom groups [25–27].

The conventional wisdom of β-relaxation is from the depth of local basins of the PEL [24] while omitting another important aspect—the width of the PEL, or the multiplicity of pathways in the sense of entropy [28–30]. Omitting entropy is inadequate. It may lead to incomplete descriptions of β-relaxation. For example, a single-barrier description cannot be straightforwardly associated with the experimentally observed wide frequency domain of β-relaxation spanning up to five to six orders of magnitudes [7,8]. In contrast, there are only two to three orders of magnitude in the frequency of α-relaxation [12,31,32]. From a structural perspective, the structural rearrangement is usually collective, which is stabilized by configurational entropy via structural ordering [33]. Therefore, clarifying the role of entropy played in β-relaxation is critical yet little touched.

Two challenges to understanding β-relaxation remain. One is that *in situ* experimental observation is hindered by extremely fine spatiotemporal resolution requirement [2]. The other is that the timescale of classic molecular dynamics (MD) is several orders of magnitude shorter than that of experiments [7,8]. Other saddle point exploration methods like the activation-relaxation technique (ART) can enumerate possible activation energies at 0 K [34–36] but miss the temperature effect and hence the entropic contribution. Recently, slow dynamics simulations of the deformation and rheology of glass under experimental conditions shed light on overcoming the timescale limitation [37–39].

Here we conduct enhanced sampling of a local structural excitation in $Cu_{50}Zr_{50}$ MG via well-tempered metadynamics (WT-MetaD) simulations [40,41] at the experimentally relevant temperature range of 200–450 K and experimentally relevant timescales, which is usually a forbidden regime for classic MD. A strongly entropic effect is uncovered via such slow dynamics modelings, which may contribute a prefactor of several orders of magnitude to the absolute frequency of

*Present address: Department of Statistics, University of Chicago, Chicago, Illinois 60637, USA.

†yjwang@imech.ac.cn

β-relaxation. The origin of activation entropy is rationalized in terms of the anharmonic feature of the local potential energy basin.

II. WELL-TEMPERED METADYNAMICS

We perform well-tempered metadynamics [40,41] samplings via the COLVARS package [42] implemented in the LAMMPS code on an archetypical binary $Cu_{50}Zr_{50}$ metallic glass model containing 4000 atoms interacting with the Finnis-Sinclair embedded-atom method empirical potential [43]. The glass is prepared by gradual quenching from an equilibrium liquid at 2000 K to the targeted temperatures with a cooling rate of 10^{10} K/s, plus a sub-T_g annealing at 700 K for 500 ns. The classic MD time step $\Delta t = 2$ fs. MD simulations are performed in an isothermal-isobaric ensemble with periodic boundary conditions applied in all three directions.

Then we switch to a canonical ensemble to perform the well-tempered metadynamics in order to boost a rare event—local structural excitation or β-relaxation—which usually experiences essential nonaffine displacements. As such we use the root-mean-square displacement (RMSD) of a group of atoms with respect to their reference positions as the collective variable (CV) to distinguish the energy minimum, saddle, and final configurations, which is a crucial requisite of a physically sound CV. The RMSD is formulated as

$$\mathrm{RMSD}\left(\{\mathbf{X}_i(t)\}, \{\mathbf{X}_i^{\mathrm{ref}}\}\right) = \sqrt{\frac{1}{N}\sum_{i=1}^{N}\left|U[\mathbf{X}_i(t)-\mathbf{X}_{\mathrm{cog}}(t)]-\left(\mathbf{X}_i^{\mathrm{ref}}-\mathbf{X}_{\mathrm{cog}}^{\mathrm{ref}}\right)\right|^2}, \tag{1}$$

where N is the number of sampled atoms and U represents an optimal rotation from the reference coordinates $\{\mathbf{X}_i^{\mathrm{ref}}\}$ to the instantaneous positions $\{\mathbf{X}_i(t)\}$ at time t. $\mathbf{X}_{\mathrm{cog}}(t)$ and $\mathbf{X}_{\mathrm{cog}}^{\mathrm{ref}}$ are the corresponding centers of geometry. RMSD is a displacement quantity that is similar to the nonaffine squared displacement D^2_{min} but easier to implement in metadynamics. The bias potential ΔV is deposited every 1000 MD steps, with a CV width of 0.35 Å. A fictive temperature $\Delta T = 2700$ K is used to decay the adding rate of the bias potential which starts with Gaussian height from 0.002 to 0.03 eV, depending on the depths of free-energy basins.

An example of WT-MetaD sampling of β-relaxation at 300 K is shown in Fig. 1. Figure 1(a) shows two jumps in the CV trajectory besides thermal fluctuation. The first jump corresponds to a looplike motion, which is one of the basic mechanisms of β-relaxation [23]. Here we deem it the major event. The second jump indicates a pair exchange. Reminiscence of the bias potential [inset of Fig. 1(b)] reproduces the original free-energy profile, from which the Helmholtz activation free energy $\Delta F(T)$ is estimated as the energy deference between the initial minimum and saddle configuration at temperature T. Local minima at 0.25 and 1.46 Å and a saddle point at 1.05 Å demonstrate the validity of RMSD as an effective CV in describing β-relaxation.

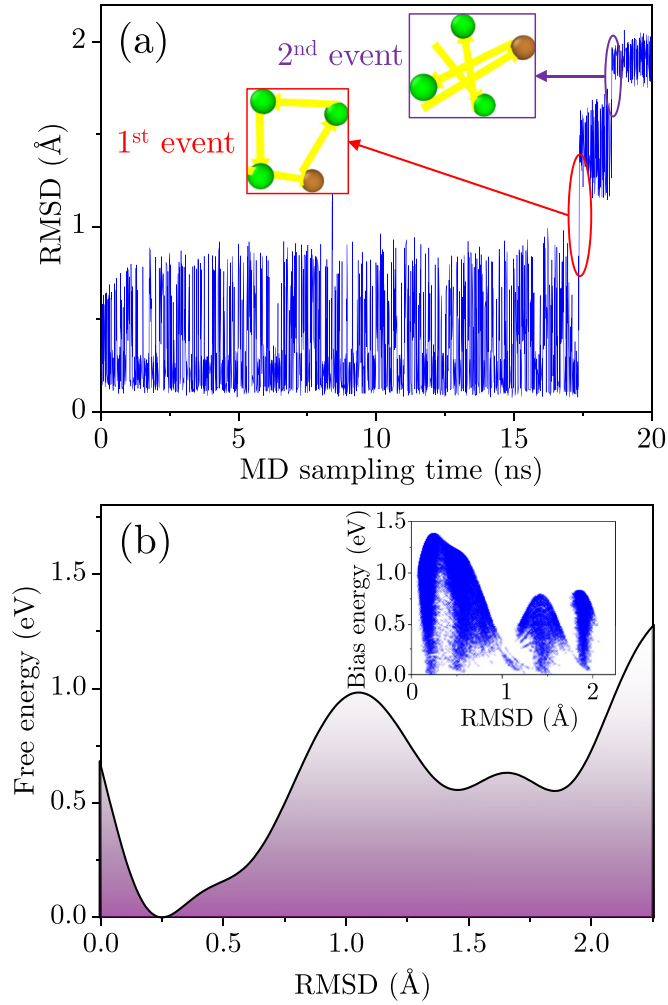

FIG. 1. WT-MetaD sampling of β-relaxation. (a) Time evolution of RMSD. The insets show the first two events, indicated by the sudden jump in CV. Only the atoms with displacement larger than 2 Å are shown. Green and bronze spheres represent Zr and Cu atoms, respectively. The arrows denote the displacement vectors. (b) Free-energy profile versus RMSD. The inset shows the bias potential.

Then the frequency of β-relaxation is calculated according to transition state theory (TST) [44],

$$\nu = \nu_0 \exp\left(-\frac{\Delta F(T)}{k_{\mathrm{B}}T}\right), \tag{2}$$

where k_{B} is Boltzmann's constant. $\nu_0 = 2 \times 10^{12}$ Hz is an attempt frequency derived as the curvature of the initial energy minimum. Considering activation entropy ΔS, ΔF is further expressed as

$$\Delta F(T) = \Delta Q - T\Delta S, \tag{3}$$

with ΔQ being activation energy at $T = 0$ K and null pressure.

In addition to metadynamics at finite temperature, the exhaustive exploration of possible saddle configurations of the same group of atoms at 0 K is conducted with ART [34–36], which is capable of highly efficient exploration of local activation events and deducing a complete distribution of activation

energies. The details of ART calculations were reported in our previous studies [45,46].

III. CONVERGENCE OF A FREE-ENERGY BARRIER TO CLUSTER SIZE

Before extensive sampling of the free-energy profiles, there is still a question left, which is how large the perturbed atom cluster should be to represent a physically relevant β-relaxation, as a local structural rearrangement may involve a few to several hundred atoms, depending on the feature of local structures [47]. To test the convergence of radial distance, several cutoff radiuses of the boosted clusters are chosen according to the characteristic positions of the radial distribution function (RDF), as shown in Fig. 2(a). The arithmetic free-energy barrier $\overline{\Delta F}$ after 50 independent samplings for each cluster size, and the effective frequency based on Eq. (3) is shown in Fig. 2(b). Here we take the case of 300 K as an example. The atom groups are centered on a Cu atom. Once the cutoff distance is larger than 4.0 Å (including 12 atoms), the frequency starts to increase sharply, which indicates the artificial introduction of a soft mechanism other than the surveyed local excitation. Therefore, we choose the atom group with a cutoff distance of 4.0 Å in following the samplings.

IV. RESULTS

A. Temperature-dependent activation energy

The raw data and box-and-whisker plot of $\Delta F(300\ \mathrm{K})$ are summarized in Fig. 3(a) with respect to sampling numbers. The mean value and standard deviation become stable after 50 samplings. By comparing the histograms after 50 and 100 samplings, shown in Figs. 3(b) and 3(c), we believe that 50 samplings capture the key features of barrier distribution.

For experimentally relevant temperatures ranging from 200 to 450 K, the histograms of ΔF are illustrated in Fig. 4(a). Several features can be drawn from the distribution. First, the distribution becomes narrower as temperature increases, indicating reduced dynamic heterogeneity, which is in agreement with the consensus from experiments. Second, the spectra follow a log-normal distribution, which has been widely assumed from theoretical perspectives [48,49] and verified experimentally by the distribution of local plastic strains in steels recently [50]. We report on the distribution of the free-energy barrier at finite temperature, whereas the 0 K case is what is usually discussed [47,49,51]. Last but not the least, the distribution of activation free energy shifts to smaller values at higher temperature, suggesting an entropic effect.

Yet mapping the spectrum to a physically sound mean-field-sense effective ΔF_{eff} is nontrivial. If one writes the probability distribution function as $P(\Delta F)$, then there are two ways to extract a single-value barrier [49,52]. One is a parallel mechanism where the total frequency is the summation of individual frequencies (or probabilities), i.e., $\exp(-\frac{\overline{\Delta F}}{k_{\mathrm{B}}T}) = \int_0^\infty P(\Delta F)\exp(-\frac{\Delta F}{k_{\mathrm{B}}T})d\Delta F$. Hence, the parallel single barrier

$$\Delta F_{\mathrm{para}} = -k_{\mathrm{B}}T\ln\left[\int_0^\infty P(\Delta F)\exp\left(-\frac{\Delta F}{k_{\mathrm{B}}T}\right)d\Delta F\right]. \quad (4)$$

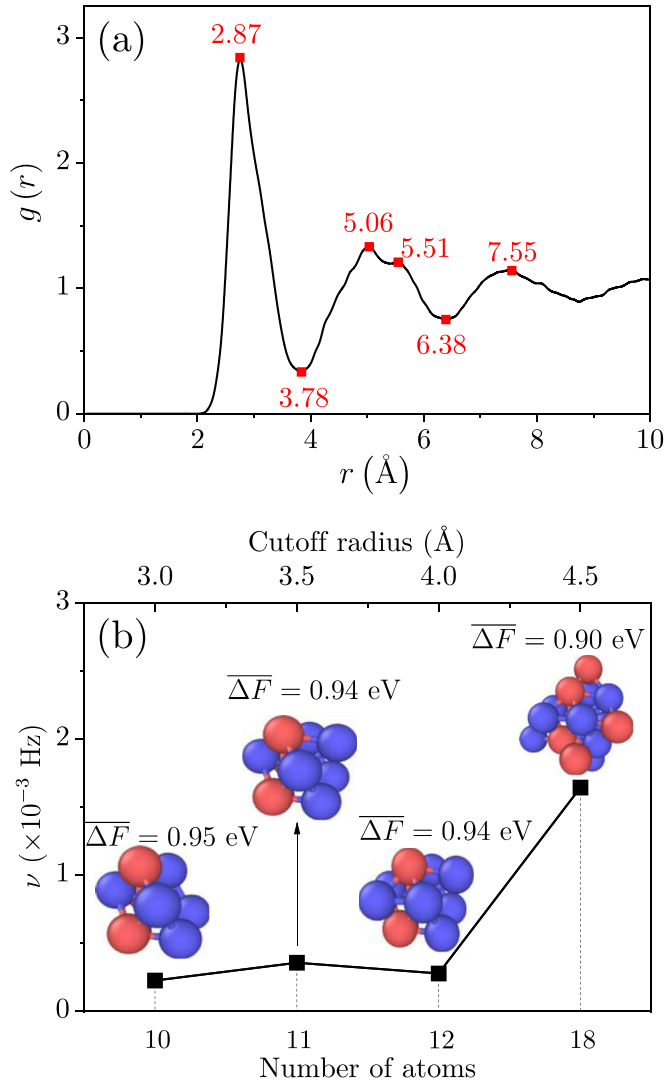

FIG. 2. Dependence of frequency and activation free energy on the size of perturbed atom groups. (a) RDF of the glass model. Several characteristic positions are labeled. (b) The predicted frequency as a function of the sampled cluster size. Once the cutoff distance is larger than 4 Å (including 12 atoms), the frequency starts to increase sharply, which indicates artificial introduction of a softer mechanism other than the surveyed local structural excitation of looplike motion. The insets denote the perturbed clusters along with their average activation free energy.

The parallel mechanism assumes that low-barrier channels are topologically connected and thus gives rise to a lower bound of effective barrier, i.e., an upper bound of effective frequency.

The other is a sequential mechanism where the total time is the summation of individuals, i.e., $\exp(\frac{\overline{\Delta F}}{k_{\mathrm{B}}T}) = \int_0^\infty P(\Delta F)\exp(\frac{\Delta F}{k_{\mathrm{B}}T})d\Delta F$, so that the sequential single barrier

$$\Delta F_{\mathrm{seq}} = k_{\mathrm{B}}T\ln\left[\int_0^\infty P(\Delta F)\exp\left(\frac{\Delta F}{k_{\mathrm{B}}T}\right)d\Delta F\right]. \quad (5)$$

The sequential mechanism assumes the activation channels are interrupted by high-barrier walls and thus defines an upper

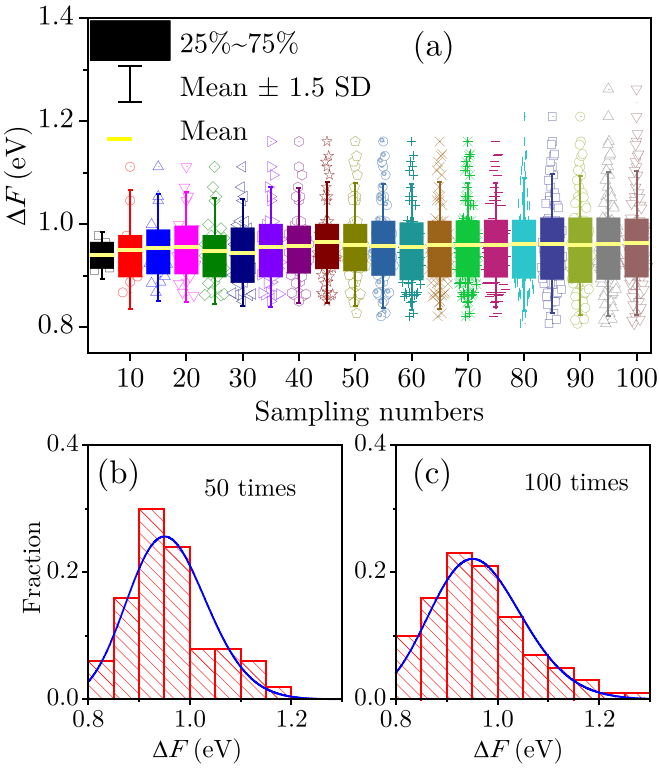

FIG. 3. Convergence of activation free energy with respect to sampling number. (a) Box-and-whisker plot of ΔF up to 100 samplings. (b) and (c) Barrier spectra after 50 and 100 samplings, respectively. The curves denote log-normal fits.

bound for the effective barrier and a lower bound for the frequency.

The remaining problem is to assign an effective single free-energy barrier that can be calibrated by experiments—the frequency of β-relaxation. For a first approximation, we take the effective activation free energy as the arithmetic mean of parallel and sequential single barriers, i.e.,

$$\Delta F_{\text{eff}} = \tfrac{1}{2}(\Delta F_{\text{para}} + \Delta F_{\text{seq}}). \tag{6}$$

Finally, the temperature-dependent ΔF of different mechanisms are shown in Figs. 4(c)–4(e). The slope of the linear fit yields activation entropy

$$\Delta S = -\frac{\partial \Delta F(T)}{\partial T}. \tag{7}$$

B. The role of activation free energy in β-relaxation

A strongly entropic effect of β-relaxation is noticed in Figs. 4(c)–4(e). Quantitatively, $\Delta S_{\text{para}} = 5.8k_{\text{B}}$ for the parallel mechanism, $\Delta S_{\text{seq}} = 23.9k_{\text{B}}$ for the sequential mechanism, and $\Delta S_{\text{eff}} = 14.8k_{\text{B}}$ for the mixing mechanism. The combination of Eqs. (2) and (3) quantifies the role of activation entropy, i.e.,

$$\nu = \nu_0 \exp\left(\frac{\Delta S}{k_{\text{B}}}\right) \exp\left(-\frac{\Delta Q}{k_{\text{B}} T}\right). \tag{8}$$

With the estimated activation energy, we now have the opportunity to quantitatively examine the role of activation entropy in β-relaxation in MGs. First, activation entropy

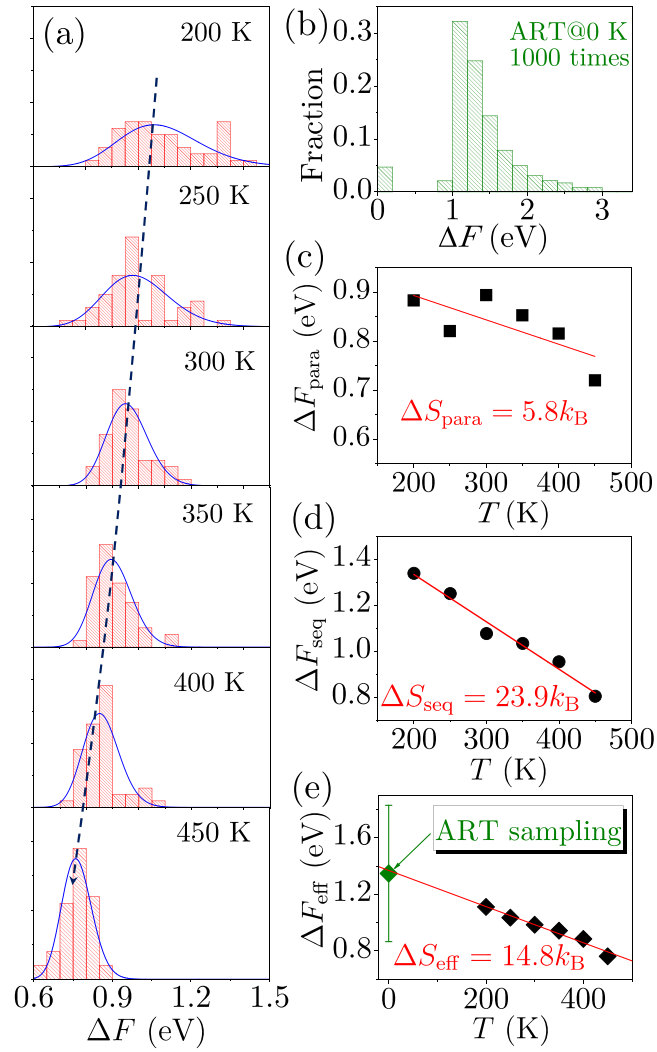

FIG. 4. Temperature dependence of activation free energy. (a) From top to bottom, the barrier spectra from 200 to 450 K. The curves represent log-normal fits. A dashed curve across the panels indicates decreased $\Delta F(T)$ with increasing T. (b) Spectrum of activation energy at 0 K via ART. (c)–(e) Temperature-dependent barrier by assuming a parallel mechanism ΔF_{para}, sequential mechanism ΔF_{seq}, and effective mechanism ΔF_{eff}, respectively. The rhombus symbol in (e) denotes ART data.

accelerates the β-relaxation frequency. For instance, the effective $\Delta S_{\text{eff}} = 14.8k_{\text{B}}$ contributes a multiplication factor $\exp(\Delta S/k_{\text{B}})$ of six orders of magnitude to the frequency. Therefore, in the rate equation formulated by Eq. (2), besides the conventional activation energy's contribution, the activation energy term cannot be dismissed in the determination of the frequency.

Next, the activation entropy indicates a collective nature of β-relaxation. Here we find the entropic effect is pronounced for the present looplike motion involving only four atoms. For comparison, the activation entropy of a more collective dislocation behavior in crystal is up to several tens of k_{B} [53]; however, for the less collective lattice [54] or grain boundary diffusion [55], the activation entropy is negligible or even negative. Therefore, one may anticipate an even stronger

entropic effect in a larger β-relaxation process involving tens of atoms [47].

Then, the finite value of the activation entropy signifies the multiplicity of activation pathways of a β event. Dynamic heterogeneity is frequently found in amorphous materials, which is thought to be from the wide distribution of relaxation times attributed to local structural heterogeneity. Here we further clarify an entropic effect for a specific looplike event (i.e., the deformation pattern is fixed). Therefore, the multiplicity nature of the relaxation pathways of local structural excitations also leads to a spectrum of activation free energies. This could be a hidden mechanism for the wide domain frequency of β-relaxation in MGs.

Finally, the activation entropy implies the topological nature of a local energy basin in the PEL of disordered materials. If the local basin is anharmonic, the normal modes of the inherent structures vary with temperature, contributing to different vibrational features and thus the entropic effect. The origin of the entropic effect will be discussed further in the remainder of the present work. Therefore, one may postulate that the local topology of the energy basin may be a signature of the difficulty of β-relaxation. Strong anharmonicity may be associated with a shallow basin.

C. Connection to experiment

To benchmark the WT-MetaD samplings and the validity of activation entropy, we conduct an exhaustive exploration of activation energies of the same group of atoms at 0 K via ART. The histogram of 1000 ART explorations is displayed in Fig. 4(b). Figure 4(e) shows that the extrapolation of $\Delta F_{\rm eff}(T)$ to 0 K, which yields activation energy from WT-MetaD samplings, is in good agreement with the average activation energy $\langle \Delta Q \rangle = 1.35$ eV from ART.

Taking entropy into consideration, we have an opportunity to compare enhanced sampling of β-relaxation with dynamic mechanical spectroscopy (DMS) experiments. Figure 5 is the Arrhenius plot of frequency against reciprocal temperature for both simulations and experimental MGs, including $La_{68.5}Ni_{16}Al_{16}Co_{1.5}$ [17,27,56], $Pd_{40}Ni_{10}Cu_{30}P_{20}$ [57], and the present experiment on $Cu_{50}Zr_{50}$. The metadynamics samplings are in agreement with most of the experiments, especially those measured in a similar temperature range with simulations. The shaped regime bounded by the parallel frequency $\nu_{\rm para}$ and sequential frequency $\nu_{\rm seq}$ clearly demonstrates the dynamical heterogeneity of β-relaxation, which is a supplement to the single-barrier scenario of DMS experiment.

An interesting observation is from the direct comparison of experimental and simulated frequencies of β-relaxation in $Cu_{50}Zr_{50}$. In experiment, the mean-field activation energy $\Delta E_\beta = 1.41 \pm 0.05$ eV, which is from an apparent Arrhenius relationship

$$f = f_0 \exp\left(-\frac{\Delta E_\beta}{k_{\rm B}T}\right), \tag{9}$$

where f is the frequency [namely, ν in Eq. (2)] and f_0 is a constant. Comparing Eqs. (8) and (9), one has $\Delta E_\beta = \Delta Q$ and $f_0 = \nu_0 \exp\left(\frac{\Delta S}{k_{\rm B}}\right)$. The seemingly parallel Arrhenius lines for $Cu_{50}Zr_{50}$ indicate that DMS and metadynamics coincidentally have identical activation energies. In detail, metadynamics

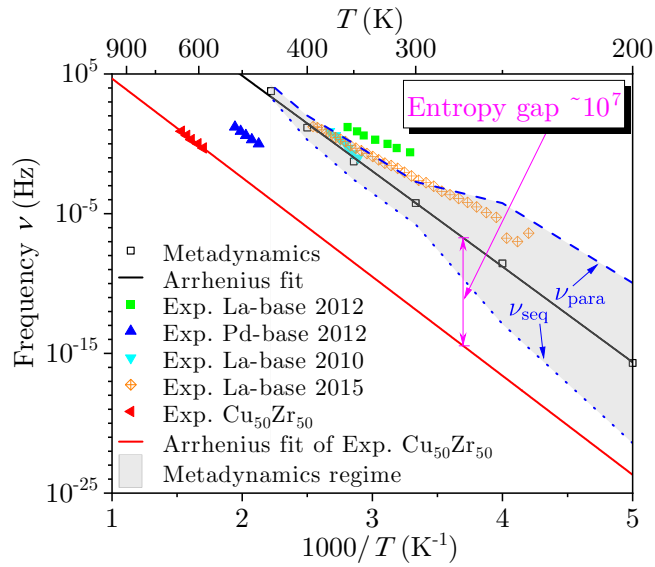

FIG. 5. Arrhenius plot of the occurring frequency of β-relaxation from well-tempered metadynamics in comparison with experimental data, including $La_{68.5}Ni_{16}Al_{14}Co_{1.5}$ [17,27,56] and $Pd_{40}Ni_{10}Cu_{30}P_{20}$ [57] in the literature and $Cu_{50}Zr_{50}$ in the present work.

predict $\Delta Q = 1.36 \pm 0.03$ eV, which indeed resembles the experimental value ΔE_β. They also match the ART data $\langle \Delta Q \rangle = 1.35$ eV. However, one cannot claim metadynamics capture all features of experiment since simulations deal with a specific form of activation, while DMS is an equivalent expression with contribution from all possible forms of excitations.

Nevertheless, the samplings do provide physical insight into β-relaxation. The intercept of the Arrhenius fit gives the activation entropy, $\ln \nu_0 + \Delta S/k_{\rm B}$. Following the above strategy, surprising data $\Delta S \simeq -k_{\rm B}$ for experimental $Cu_{50}Zr_{50}$ is derived via the intercept of the Arrhenius fit to the high-temperature limit (red line in Fig. 5). In this case, there is almost no entropic effect, in analogy to that of lattice diffusion in crystal [54]. This is possibly attributed to the thermodynamic conditions of DMS—high temperature near the glass transition $T_{\rm g} = 695$ K. For other glasses that are measured at lower temperatures far below $T_{\rm g}$, large activation entropy emerges as metadynamics predicted.

V. DISCUSSION: ORIGIN OF ACTIVATION ENTROPY

In principle, the activation entropy arises from either the vibrational or configurational entropy difference between the saddle and minimum energy configurations. Since the mode of structural rearrangement is fixed in the sampling, the former contribution is the major factor. The physical meaning of activation entropy is clear in the framework of TST, which expresses $\nu_0 \exp\left(\frac{\Delta S}{k_{\rm B}}\right) = \frac{\prod_i^{3N} \omega_i^{\rm ini}(T)}{\prod_i^{3N-1} \omega_i^{\rm sad}(T)}$, where $\omega_i^{\rm ini}(T)$ and $\omega_i^{\rm sad}(T)$ are the non-negative normal-mode frequencies of the initial energy minimum and saddle point configurations, respectively, of the surveyed inherent structure inherited from the parental temperature $T_{\rm P}$ (Fig. 6). If the shape of the local energy basin is thoroughly harmonic, then the

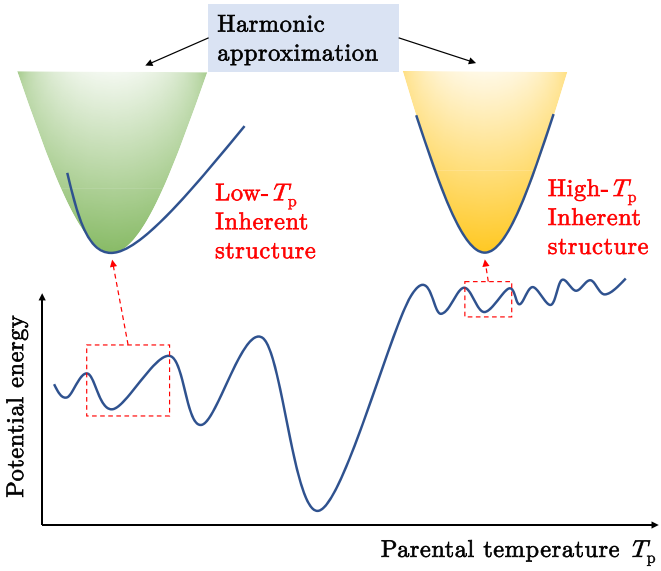

FIG. 6. Schematic illustration of the topological feature of PEL in terms of the anharmonic effect.

temperature-independent ν_0 already represents a good approximation of the attempting frequency. Thus, no activation entropy exists. However, if strong anharmonic component exists in the local basin, thermal or saddle softening (smaller ω_i^{sad}) occurs and gives rise to an entropic effect with a remarkable magnitude of ΔS. Since the parental temperature of metadynamics samples is low, an obvious entropic effect exists which is consistent with the DMS measurement of La-based glasses at relatively low temperature. However, the local basins of the inherent structure of experimental CuZr glass at around 600 K are possibly more harmonic; therefore, the activation entropy is trivial.

We further explain the entropic effect of β-relaxation due to anharmonicity of the local basin, which is schematically displayed in Fig. 6. At low parental temperature T_P where the stable inherent structure is inherited, the local basin where β-relaxation resides is strongly anharmonic. Therefore, the normal-mode frequency is temperature dependent. As a result, there is a vibrational entropic effect since vibrational frequencies are affected by temperature at either the initial energy minimum or the saddle state. However, for the inherent structure prepared at high parental temperature (e.g., a supercooled liquid), the local basin has been well described by the harmonic approximation, and therefore, the vibrational entropy is negligible. The topological feature of the PEL in terms of the harmonic approximated is verified by the WT-MetaD samplings at ambient temperature and the DMS experiment at high temperature.

Combining the metadynamics and experimental results in Fig. 5 shows that the entropic effect of local excitation is large in the deep glass state, while in the supercooled or liquid state, the contribution of vibrational activation entropy vanishes. In this regime, the configurational entropy fluctuation governs the dynamics. This picture was verified recently by successful separation of configurational and vibrational entropy in glass-forming alloys with both an inelastic neutron scattering experiment [58] and molecular dynamics [59,60].

VI. CONCLUSION

Overall, enhanced samplings over experimental timescales exploit the spectrum of temperature-dependent activation free energy for the β-relaxation in metallic glass. The free-energy barrier distribution provides insight into the critical role of activation entropy in the β-relaxation. The magnitude of activation entropy is estimated to be more than $10k_B$, which may contribute significantly, with a multiplication factor of several orders of magnitude, to the absolute frequency. This work also provides a theoretical basis for understanding why the β-relaxation frequency domain in glasses is usually much wider than that of α-relaxation. The entropic effect provides a complementary view to the usual idea of β-relaxation from an energetic perspective. It is a step toward understanding the multiplicity of activation pathways, beyond the insight of difficulty in activation. In other words, it initiates further discussions on the nature of the local PEL width beyond the current knowledge established from the saddle configuration height on the PEL of disordered materials.

ACKNOWLEDGMENTS

This work is financially supported by the NSFC (Grants No. 12072344, No. 11672299, and No. 11790292), the National Key Research and Development Program of China (Grants No. 2017YFB0702003 and No. 2017YFB0701502), and the Youth Innovation Promotion Association of the Chinese Academy of Sciences (Grant No. 2017025).

[1] H. W. Sheng, W. K. Luo, F. M. Alamgir, J. M. Bai, and E. Ma, Atomic packing and short-to-medium-range order in metallic glasses, Nature (London) **439**, 419 (2006).

[2] A. Hirata, L. J. Kang, T. Fujita, B. Klumov, K. Matsue, M. Kotani, A. R. Yavari, and M. W. Chen, Geometric frustration of icosahedron in metallic glasses, Science **341**, 376 (2013).

[3] E. D. Cubuk, R. J. S. Ivancic, S. S. Schoenholz, D. J. Strickland, A. Basu, Z. S. Davidson, J. Fontaine, J. L. Hor, Y.-R. Huang, Y. Jiang, N. C. Keim, K. D. Koshigan, J. A. Lefever, T. Liu, X.-G. Ma, D. J. Magagnosc, E. Morrow, C. P. Ortiz, J. M. Rieser, A. Shavit *et al.*, Structure-property relationships from universal signatures of plasticity in disordered solids, Science **358**, 1033 (2017).

[4] V. Bapst, T. Keck, A. Grabska-Barwińska, C. Donner, E. D. Cubuk, S. S. Schoenholz, A. Obika, A. W. R. Nelson, T. Back, D. Hassabis, and P. Kohli, Unveiling the predictive power of static structure in glassy systems, Nat. Phys. **16**, 448 (2020).

[5] G. P. Johari and M. Goldstein, Viscous liquids and the glass transition. II. Secondary relaxations in glasses of rigid molecules, J. Chem. Phys. **53**, 2372 (1970).

[6] K. Ngai, *Relaxation and Diffusion in Complex Systems* (Springer, New York, 2011).

[7] H. B. Yu, W. H. Wang, and K. Samwer, The β relaxation in metallic glasses: An overview, Mater. Today **16**, 183 (2013).

[8] H. B. Yu, W. H. Wang, H. Y. Bai, and K. Samwer, The β-relaxation in metallic glasses, Natl. Sci. Rev. **1**, 429 (2014).

[9] U. Schneider, R. Brand, P. Lunkenheimer, and A. Loidl, Excess Wing in the Dielectric Loss of Glass Formers: A Johari-Goldstein β Relaxation? Phys. Rev. Lett. **84**, 5560 (2000).

[10] K. Geirhos, P. Lunkenheimer, and A. Loidl, Johari-Goldstein Relaxation Far Below T_g: Experimental Evidence for the Gardner Transition in Structural Glasses? Phys. Rev. Lett. **120**, 085705 (2018).

[11] T. Blochowicz and E. A. Rössler, Beta Relaxation versus High Frequency Wing in the Dielectric Spectra of a Binary Molecular Glass Former, Phys. Rev. Lett. **92**, 225701 (2004).

[12] A. Zaccone, Relaxation and vibrational properties in metal alloys and other disordered systems, J. Phys.: Condens. Matter **32**, 203001 (2020).

[13] S. V. Ketov, Y. H. Sun, S. Nachum, Z. Lu, A. Checchi, A. R. Beraldin, H. Y. Bai, W. H. Wang, D. V. Louzguine-Luzgin, M. A. Carpenter, and A. L. Greer, Rejuvenation of metallic glasses by non-affine thermal strain, Nature (London) **524**, 200 (2015).

[14] J. Pan, Y. P. Ivanov, W. H. Zhou, Y. Li, and A. L. Greer, Strain-hardening and suppression of shear-banding in rejuvenated bulk metallic glass, Nature (London) **578**, 559 (2020).

[15] C. A. Schuh, T. C. Hufnagel, and U. Ramamurty, Mechanical behavior of amorphous alloys, Acta Mater. **55**, 4067 (2007).

[16] J. C. Ye, J. Lu, C. T. Liu, Q. Wang, and Y. Yang, Atomistic free-volume zones and inelastic deformation of metallic glasses, Nat. Mater. **9**, 619 (2010).

[17] H. B. Yu, X. Shen, Z. Wang, L. Gu, W. H. Wang, and H. Y. Bai, Tensile Plasticity in Metallic Glasses with Pronounced β Relaxations, Phys. Rev. Lett. **108**, 015504 (2012).

[18] B. Cui, J. Yang, J. Qiao, M. Jiang, L. Dai, Y.-J. Wang, and A. Zaccone, Atomic theory of viscoelastic response and memory effects in metallic glasses, Phys. Rev. B **96**, 094203 (2017).

[19] K. L. Ngai, Relation between some secondary relaxations and the α relaxations in glass-forming materials according to the coupling model, J. Chem. Phys. **109**, 6982 (1998).

[20] S. Sastry, P. G. Debenedetti, and F. H. Stillinger, Signatures of distinct dynamical regimes in the energy landscape of a glass-forming liquid, Nature (London) **393**, 554 (1998).

[21] K. L. Ngai and S. Capaccioli, Relation between the activation energy of the Johari-Goldstein β relaxation and T_g of glass formers, Phys. Rev. E **69**, 031501 (2004).

[22] Y. H. Liu, T. Fujita, D. P. B. Aji, M. Matsuura, and M. W. Chen, Structural origins of Johari-Goldstein relaxation in a metallic glass, Nat. Commun. **5**, 3238 (2014).

[23] H.-B. Yu, R. Richert, and K. Samwer, Structural rearrangements governing Johari-Goldstein relaxations in metallic glass, Sci. Adv. **3**, e1701577 (2017).

[24] P. G. Debenedetti and F. H. Stillinger, Supercooled liquids and the glass transition, Nature (London) **410**, 259 (2001).

[25] A. S. Argon, Plastic deformation in metallic glasses, Acta Metall. **27**, 47 (1979).

[26] M. L. Falk and J. S. Langer, Dynamics of viscoplastic deformation in amorphous solids, Phys. Rev. E **57**, 7192 (1998).

[27] H. B. Yu, W. H. Wang, H. Y. Bai, Y. Wu, and M. W. Chen, Relating activation of shear transformation zones to β relaxations in metallic glasses, Phys. Rev. B **81**, 220201(R) (2010).

[28] M. Ozawa, A. Ikeda, K. Miyazaki, and W. Kob, Ideal Glass States Are Not Purely Vibrational: Insight from Randomly Pinned Glasses, Phys. Rev. Lett. **121**, 205501 (2018).

[29] L. Berthier, P. Charbonneau, D. Coslovich, A. Ninarello, M. Ozawa, and S. Yaida, Configurational entropy measurements in extremely supercooled liquids that break the glass ceiling, Proc. Natl. Acad. Sci. USA **114**, 11356 (2017).

[30] Y.-J. Wang, M. Zhang, L. Liu, S. Ogata, and L. H. Dai, Universal enthalpy-entropy compensation rule for the deformation of metallic glasses, Phys. Rev. B **92**, 174118 (2015).

[31] J. C. Qiao, Q. Wang, J. M. Pelletier, H. Kato, R. Casalini, D. Crespo, E. Pineda, Y. Yao, and Y. Yang, Structural heterogeneities and mechanical behavior of amorphous alloys, Prog. Mater. Sci. **104**, 250 (2019).

[32] W.-H. Wang, Dynamic relaxations and relaxation-property relationships in metallic glasses, Prog. Mater. Sci. **106**, 100561 (2019).

[33] H. Tanaka, H. Tong, R. Shi, and J. Russo, Revealing key structural features hidden in liquids and glasses, Nat. Rev. Phys. **1**, 333 (2019).

[34] G. T. Barkema and N. Mousseau, Event-Based Relaxation of Continuous Disordered Systems, Phys. Rev. Lett. **77**, 4358 (1996).

[35] R. Malek and N. Mousseau, Dynamics of Lennard-Jones clusters: A characterization of the activation-relaxation technique, Phys. Rev. E **62**, 7723 (2000).

[36] E. MacHado-Charry, L. K. Béland, D. Caliste, L. Genovese, T. Deutsch, N. Mousseau, and P. Pochet, Optimized energy landscape exploration using the *ab initio* based activation-relaxation technique, J. Chem. Phys. **135**, 034102 (2011).

[37] P. Cao, M. P. Short, and S. Yip, Understanding the mechanisms of amorphous creep through molecular simulation, Proc. Natl. Acad. Sci. USA **114**, 13631 (2017).

[38] P. Cao, M. P. Short, and S. Yip, Potential energy landscape activations governing plastic flows in glass rheology, Proc. Natl. Acad. Sci. USA **116**, 18790 (2019).

[39] A. Ninarello, L. Berthier, and D. Coslovich, Models and Algorithms for the Next Generation of Glass Transition Studies, Phys. Rev. X **7**, 021039 (2017).

[40] A. Barducci, G. Bussi, and M. Parrinello, Well-Tempered Metadynamics: A Smoothly Converging and Tunable Free-Energy Method, Phys. Rev. Lett. **100**, 020603 (2008).

[41] G. Bussi and A. Laio, Using metadynamics to explore complex free-energy landscapes, Nat. Rev. Phys. **2**, 200 (2020).

[42] G. Fiorin, M. L. Klein, and J. Hénin, Using collective variables to drive molecular dynamics simulations, Mol. Phys. **111**, 3345 (2013).

[43] M. I. Mendelev, M. J. Kramer, R. T. Ott, D. J. Sordelet, D. Yagodin, and P. Popel, Development of suitable interatomic potentials for simulation of liquid and amorphous Cu–Zr alloys, Philos. Mag. **89**, 967 (2009).

[44] H. Eyring, The activated complex in chemical reactions, J. Chem. Phys. **3**, 107 (1935).

[45] D. Wei, J. Yang, M.-Q. Jiang, B.-C. Wei, Y.-J. Wang, and L.-H. Dai, Revisiting the structure-property relationship of metallic glasses: Common spatial correlation revealed as a hidden rule, Phys. Rev. B **99**, 014115 (2019).

[46] D. Han, D. Wei, P.-H. Cao, Y.-J. Wang, and L.-H. Dai, Statistical complexity of potential energy landscape as a dynamic signature of the glass transition, Phys. Rev. B **101**, 064205 (2020).

[47] Y. Fan, T. Iwashita, and T. Egami, How thermally activated deformation starts in metallic glass, Nat. Commun. **5**, 5083 (2014).

[48] P. M. Derlet and R. Maaß, Linking high- and low-temperature plasticity in bulk metallic glasses II: use of a log-normal barrier energy distribution and a mean-field description of high-temperature plasticity, Philos. Mag. **94**, 2776 (2014).

[49] Y. Fan, T. Iwashita, and T. Egami, Energy landscape-driven non-equilibrium evolution of inherent structure in disordered material, Nat. Commun. **8**, 15417 (2017).

[50] A. Tang, H. Liu, G. Liu, Y. Zhong, L. Wang, Q. Lu, J. Wang, and Y. Shen, Lognormal Distribution of Local Strain: A Universal Law of Plastic Deformation in Material, Phys. Rev. Lett. **124**, 155501 (2020).

[51] Y. Fan, T. Iwashita, and T. Egami, Crossover from Localized to Cascade Relaxations in Metallic Glasses, Phys. Rev. Lett. **115**, 045501 (2015).

[52] Y.-J. Wang, J.-P. Du, S. Shinzato, L.-H. Dai, and S. Ogata, A free energy landscape perspective on the nature of collective diffusion in amorphous solids, Acta Mater. **157**, 165 (2018).

[53] S. Ryu, K. Kang, and W. Cai, Entropic effect on the rate of dislocation nucleation, Proc. Natl. Acad. Sci. USA **108**, 5174 (2011).

[54] V. Milman, M. C. Payne, V. Heine, R. J. Needs, J. S. Lin, and M. H. Lee, Free Energy and Entropy of Diffusion by *Ab Initio* Molecular Dynamics: Alkali Ions in Silicon, Phys. Rev. Lett. **70**, 2928 (1993).

[55] Y.-J. Wang, G.-J. J. Gao, and S. Ogata, Atomistic understanding of diffusion kinetics in nanocrystals from molecular dynamics simulations, Phys. Rev. B **88**, 115413 (2013).

[56] Q. Wang, S. Zhang, Y. Yang, Y. Dong, C. Liu, and J. Lu, Unusual fast secondary relaxation in metallic glass, Nat. Commun. **6**, 7876 (2015).

[57] H. B. Yu, K. Samwer, Y. Wu, and W. H. Wang, Correlation between β Relaxation and Self-Diffusion of the Smallest Constituting Atoms in Metallic Glasses, Phys. Rev. Lett. **109**, 095508 (2012).

[58] H. L. Smith, C. W. Li, A. Hoff, G. R. Garrett, D. S. Kim, F. C. Yang, M. S. Lucas, T. Swan-Wood, J. Y. Y. Lin, M. B. Stone, D. L. Abernathy, M. D. Demetriou, and B. Fultz, Separating the configurational and vibrational entropy contributions in metallic glasses, Nat. Phys. **13**, 900 (2017).

[59] D. Han, D. Wei, J. Yang, H.-L. Li, M.-Q. Jiang, Y.-J. Wang, L.-H. Dai, and A. Zaccone, Atomistic structural mechanism for the glass transition: Entropic contribution, Phys. Rev. B **101**, 014113 (2020).

[60] R. Alvarez-Donado and A. Antonelli, Splitting up entropy into vibrational and configurational contributions in bulk metallic glasses: A thermodynamic approach, Phys. Rev. Research **2**, 013202 (2020).